Effect of depth of soil stratum on performance of buildings for site-specific earthquakes

P. Kamatchi [a,*], J. Rajasankar [a], Nagesh R. Iyer [a], N. Lakshmanan [a], G.V. Ramana [b], A.K. Nagpal [b]

[a] CSIR-Structural Engineering Research Centre, CSIR Campus, Taramani, Chennai 600 113, India
[b] Department of Civil Engineering, Indian Institute of Technology Delhi, Hauz Khas, New Delhi 110 016, India

ARTICLE INFO

ABSTRACT

Towards formulating guidelines for performance evaluation of buildings to site-specific earthquakes, studies are reported in literature on the effect of various critical parameters. No study is, however, reported on the effect of depth of soil stratum. In this paper, a methodology is proposed and applied for performance evaluation of buildings for site-specific earthquakes including depth of soil stratum as a parameter. The methodology integrates independent procedures meant for performance evaluation of buildings and site-specific seismic analysis. Application of the proposed methodology enables to determine performance point of a building in terms of inelastic displacement and base shear. Numerical application of the methodology is demonstrated using the particulars of Delhi region. Two typical RC buildings (B1 and B2) with significantly different inelastic behaviour, assumed to be located on soil depths ranging from 10 to 200 m are chosen for the application study. Capacity spectra of the buildings are generated from nonlinear static analysis. Studies indicate that for building B1, with elasto-plastic behaviour, the depth of soil stratum strongly influences demand on inelastic displacement compared to that on inelastic base shear. For building B2, with continuously varying inelastic behaviour, the depth of soil stratum is observed to have significant influence on both the inelastic base shear as well as inelastic displacement. Responses of the buildings are compared with that obtained based on design spectrum of Indian seismic code. For both the cases, inelastic displacements as well as inelastic base shears are underestimated by Indian seismic code for certain depths of soil stratum. Proposed methodology enables the calculation of realistic values of inelastic base shear and corresponding displacement of a building for site-specific earthquakes by considering the actual characteristics of soil stratum.

1. Introduction

New generation seismic design codes are shifting towards performance based design of buildings [1–3]. This necessitates development of methodologies for performance evaluation of designed buildings for earthquakes. In this context, provisions for inclusion of the effect of critical parameters viz., soil–structure interaction, type of foundation, nature of ground motion and soil are reported in literature [4–7]. Effect of soil amplification has been well recognised in existing seismic design codes. Indian seismic design code IS-1893-2002 Part I [8] has three distinct design spectra exclusively for soft, medium and hard soils. As an improvement over this, amplification factors based on empirical and theoretical data [9] have been introduced in International Building Code (IBC) [10] for site class A to F to take care of the behaviour in short as well as long period range. Elghazouli [11]

reported that in Eurocode (EC 8 Part 5), two types of response spectra have been proposed for five different soil conditions (Type A to E). Response spectra are identified with different soils and the expected magnitude of ground motion. Classification of site soil A to E has been made on the basis of average shear wave velocity of top 30 m soil.

Sun et al. [12] have showed that the site coefficients specified in IBC [10] are not valid for Korean Peninsula due to the large difference in the depth of bedrock and the soil stiffness profile. On extending this observation, application of the soil amplification factors specified by Borcherdt [9] to several other regions can produce results of unacceptable error. Further, building design codes are highly simplified tools and do not adequately represent any single earthquake event from a probable source for the site under consideration. It has been recommended [13] that in addition to use of codal provisions, site-specific analysis which includes generation of strong ground motion at bedrock level and propagating it through soil layers [13–15] and arriving at the design ground motions and response spectra at surface should also be carried out. On the other hand, considering the loss due to

---

collapse or cost of repair, substantial revisions are taking place in major seismic design codes to evolve next generation design procedures [16–18]. Important considerations for the revisions are to account for acceptable levels of damage to buildings in a seismic event of known characteristics and also to include the actual performance of a building at the proposed site conditions. Performance evaluation of buildings is a process which involves both the structure and soil characteristics which need proper treatment in analysis phase.

To the authors' knowledge, no methodology or a comprehensive study is reported on seismic performance evaluation of buildings for site-specific earthquakes. Despite the understanding and observation of the role of local soil on seismic wave amplification, practical design of structures is being made based on the spectra suggested by seismic design codes. Within the framework of performance evaluation of structures, design spectra act as performance objective. Besides this, design spectra also acts as demand curve in a design using conventional procedures. It is well known that the response spectra at soil surface can be significantly different from that of the bedrock response spectra due to modification of ground motion characteristics, as the wave travels through soil layers overlying the bedrock. In this background, a simple methodology is proposed and applied in this paper to evaluate the performance of buildings for site-specific earthquakes including depth of soil stratum as a parameter.

Basically, the methodology involves comparison of demand spectrum corresponding to an earthquake under the given soil condition against capacity spectrum of a building. Well-established procedures are available to evaluate the capacity spectrum of a building to a reasonable accuracy while considerable uncertainty exists in the generation of demand spectrum. In the present study, demand spectra corresponding to site-specific earthquakes are generated by carrying out the following two steps: (i) evaluation of ground response spectra using strong ground motion generated at bedrock level for a scenario earthquake and conducting a one-dimensional equivalent linear wave propagation analysis and (ii) generation of Depth Dependent Demand Spectra corresponding to the individual site conditions. More details about the methodology are described in the next section. The methodology is verified using particulars of Delhi city in India. The main reason for choosing this city is the availability of geotechnical details for successful application of the methodology. It is to the belief of authors that the proposed methodology is general and, therefore, applicable to any other region at which local soil is expected to contribute significantly to the seismic behaviour of the structure. Comparison among the computed numerical values provides valuable information about the inelastic behaviour of buildings due to the effect of local soil.

2. Methodology

Two important elements of seismic performance evaluation of buildings are demand and capacity spectra. Demand spectrum is the representation of the severity of the ground motion while capacity spectrum depicts the ability of the structure to withstand forces of specific nature. Demand spectrum has to be modified to account for lengthening of the period or increase in the damping of the structure. Proposed methodology adopts capacity spectrum method [4,19,20] to generate the demand spectrum as the method has provisions to accommodate the modifications. Fig. 1 gives the overall structure of the proposed methodology, individual steps and the sequence in which these are to be executed.

Considerable knowledge and experience exist in literature for the generation of capacity spectrum of a structure by adequately taking care of nonlinear behaviour of both concrete and reinforcing steel. State-of-the-art lies in the availability of ready-to-use software with wide range of options for modelling almost all cases that are likely to be encountered in practice. On the other hand, generation of demand spectrum by properly accounting for the nonlinear behaviour of soil at site is a challenging task. Successful generation of demand spectrum requires input on various aspects like proximity to and nature of the source of earthquake, path effects of seismic waves and local soil conditions. Due to its nature, a comprehensive methodology that can address all the important issues is essential for generation of demand spectrum.

2.1. Site-specific demand spectra

Response spectrum suggested by seismic design codes plays the role of demand spectrum for normal structures. As discussed earlier, design codes considerably simplify the actual soil conditions to suggest a maximum of three soil categories as hard rock, medium and soft soil. This is done on the basis that the seismic behaviour of such structures will not be affected much by consideration of exact variation in soil types. For critical structures, however, it is mandatory to carry out site-specific analysis to reliably ascertain their seismic performance [16–18]. Even for other structures, it is preferable to carry out a site-specific analysis to arrive at realistic demand spectrum. Site-specific analysis, however, requires considerable effort towards modelling and computations w.r.t. generation and propagation of strong ground motion through the soil strata.

2.1.1. Generation of strong ground motion

First step of the methodology is to generate strong ground motion at bedrock level. Recorded ground motion is not available for Delhi region, hence in the present study artificial strong motions are generated using stochastic model. Stochastic simulation procedure for ground motion generation based on seismological models using point source model has been proposed by Boore [21,22]. In this procedure the band limited Gaussian white noise is windowed and filtered in the time domain and transformed into frequency domain. The Fourier amplitude spectrum is scaled to the mean squared absolute spectra and multiplied by a Fourier amplitude spectrum obtained by considering source path effects. Then, the spectrum is transformed back to time domain to obtain time history of accelerations.

From the analysis of recorded ground motions, it has been reported [23] that point source models are not capable of reproducing the characteristic features of large earthquakes ($M_w > 6$) viz., long duration and radiation of less energy at low to intermediate frequencies (0.2–2 Hz). Simulation of strong ground motion from finite fault rupture has been developed by Beresnev and Atkinson [23,24]. The fault rupture plane is modelled with an array of sub-faults and the radiation from each sub-fault is modelled as a point source similar to Boore's model [21]. According to finite source model, the fault rupture initiates at the hypocenter and spreads uniformly along the fault plane radially outward with a constant rupture velocity triggering radiation from sub-faults in succession. The Fourier amplitude spectrum $A(\omega)$ of the point source of an element (sub-fault) is defined [23,24] as

$$A(\omega) = \omega^2 S(\omega) P(\omega) G(R) A_n(\omega) \tag{1}$$

where, ω is the angular frequency, $S(\omega)$ is the source function, $P(\omega)$ is the filter function for high frequency attenuation, $G(R)$ is
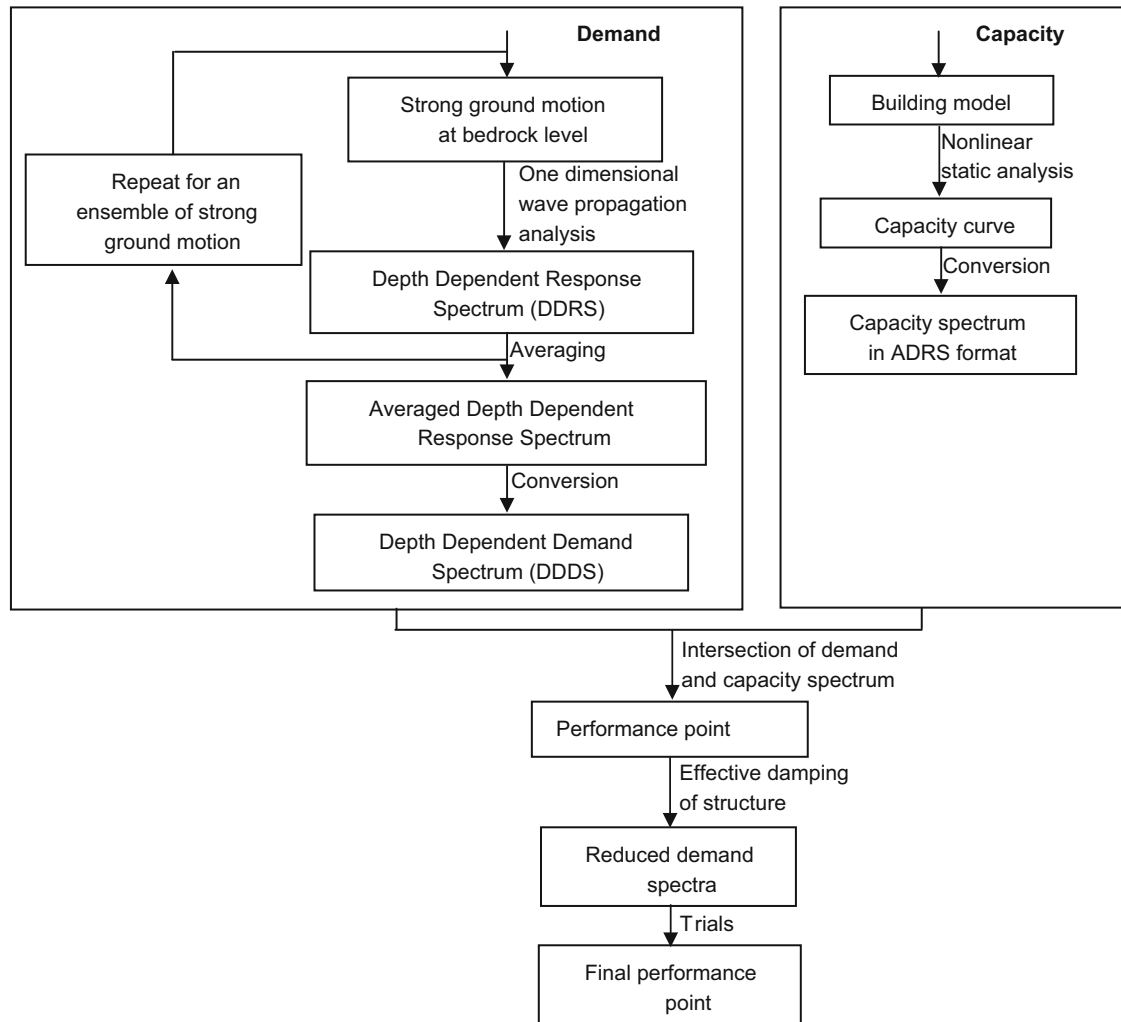
Fig. 1. Proposed methodology.

Table 1
Seismological parameters for strong motion generation.

Sl. No.	Parameters	Model/value
1	Fault orientation	Strike 300° Dip 7°
2	Stress parameter (bars)	50
3	Duration model	$1/f_c + 0.05\,R$
4	Quality factor	$508f^{0.48}$
5	Windowing function	Saragoni-Hart
6	f_{max} (Hz)	15
7	Crustal shear wave velocity (km/sec)	3.6
8	Crustal density (kN/m^3)	2.8
9	Radiation strength factor	1.4
10	Fault dimension along strike and dip (km)	240×80
11	Depth of focus (km)	16
12	No. of sub-faults	16×5
13	No. of sub-sources summed	339

F – frequency; f_c – corner frequency; f_{max}-cut off frequency; R – epi-central distance

the geometric attenuation function, $A_n(\omega)$ is an elastic whole path attenuation function.

Finite fault simulation program (FINSIM) has been widely used for the generation of ground motions of large size earthquakes [25,26] and hence has been adopted in the present study. Parameters and their values used to generate strong ground motion for the scenario earthquake are given in Table 1.

2.1.2. Generation of Depth Dependent Response Spectra (DDRS)

Recorded seismic ground motions contain source, path and site effects. Among these, the source and path effects are already accounted while generating the strong ground motion at the bedrock level in the previous step. Still site effects are required to be included in the generated ground motion in order to match it with recorded ground motions in terms of its quality. For this purpose, the next step suggested as per Fig. 1 is to generate Depth Dependent Response Spectra (DDRS) of the site by actually modelling the soil strata.

Numerical methods [27] to evaluate site response can be one-dimensional (1D), two-dimensional (2D) or three-dimensional (3D). Two- and three-dimensional analyses are carried out when the surface topography is in the form of ridges, mountains, hills (convex surfaces), valleys, and basins (concave surfaces). One-dimensional wave propagation analysis with horizontally homo-geneous and vertically varying soil medium is very powerful and hence widely used [28,29] for characterizing local soil effects. One-dimensional analysis can be either equivalent linear or nonlinear. Depending on the intensity of bedrock motion, the soil sediment undergoes linear or nonlinear strains.

Taking the above aspects into consideration, in the second step of the methodology, it is proposed to conduct an equivalent linear analysis of the wave propagation in the soil stratum to incorporate site effect. The computer program SHAKE 2000 [30] is an one-dimensional equivalent linear wave propagation

analysis program, with continuous solution to the wave equation adopted for use with transient motion through the Fast Fourier Transformation (FFT). Nonlinearity of the shear modulus and damping of the soil is accounted by using equivalent linear soil properties. Soil system is modelled to extend infinitely in horizontal direction. Each layer in the system is defined by its value of shear modulus, critical damping ratio, density and thickness which are independent of frequency. Responses in the system are caused by upward propagation of shear waves from the underlying rock formation. Ground motion at the rock layer below the soil strata is applied as rock outcrop motion.

Artificially generated strong ground motion is known to have randomness due to the inherent properties of the generation procedures. In an effort to arrive at smooth and better representation of the source, path and site effects, it is suggested to evaluate the DDRS as an average of sample of generated strong ground motion. The sample size shall be decided as a compromise between the available computational resources and the smoothness desired in the generated response spectrum. This is also shown in Fig. 1.

2.1.3. Conversion of DDRS to Depth Dependent Demand Spectra (DDDS)

After carrying out the previous step, the DDRS is obtained in the standard spectral acceleration (S_a) versus time period (T) format. This format is convenient to understand the wave amplification nature of the soil medium. However, the objective of the proposed methodology is to estimate the performance point of a building. To meet this objective, third step of the methodology is proposed to derive the Depth Dependent Demand Spectra (DDDS) in Acceleration-Displacement Response Spectra (ADRS). The derivation is proposed to be executed through [19]

$$S_{di} = \frac{T_i^2}{4\pi^2} S_{ai} g \tag{2}$$

where S_{di}=spectral displacement ordinate in m; S_{ai}=spectral acceleration ordinate in units of g; T_i=time period of the building in secs; g=acceleration due to gravity in m/s^2; i=ith point of the spectra.

By carrying out the three steps described in Sections 2.1.1–2.1.3, DDDS incorporated with the characteristics of the seismic wave behaviour at the site can be obtained. The generated DDDS is unique by considering the effects of source, path and wave amplification nature of the soil stratum.

2.2. Capacity spectrum method

2.2.1. Capacity curve through nonlinear static analysis

The overall load capacity of a structure depends on the strength and deformation capacities of its individual components. In order to determine capacities beyond the elastic limits, it is proposed to use a series of sequential elastic analyses with results from successive analysis superimposed to approximate a force–displacement capacity diagram of the overall structure. The capacity curve is to be constructed to represent the deformation corresponding to first mode response of the structure. Contribution of higher modes to the capacity curve can be included based on standard procedures [31]. Modelling the inelastic deformation capacity of beams and columns is an important task in the evaluation of capacity curve for RC buildings. In the present study, SAP2000 [32] software is used for nonlinear static analysis. Based on ATC 40 [19] guidelines, inelastic deformation properties are adopted in terms of default PMM hinge for columns and default M3 hinge for beams.

2.2.2. Conversion of capacity curve to capacity spectrum

Capacity curve of a building is obtained based on the results of nonlinear static analysis (Section 2.2.1). This is to be transformed to capacity spectrum using the spectral coordinates [19] corresponding to the first natural mode of the building. Conversion of ordinates can be effected as

$$S_{aj} = \frac{V_j/W}{\alpha_1} \tag{3}$$

$$S_{dj} = \frac{\Delta_{roof}}{PF_1 \phi_{1,roof}} \tag{4}$$

where V_j=base shear at the jth point of the capacity curve; W=weight of the building as sum of dead load and percentage live load; α_1=modal mass coefficient for the first natural mode; Δ_{roof}=roof displacement; PF_1=modal participation factor for the first natural mode; $\phi_{1,roof}$=amplitude of roof in first natural mode.

2.3. Performance point

At this stage, both the demand and capacity spectra specific to the characteristics of the building and the demand at site would have been generated. The next step of the methodology involves identification of performance point of the building. As same format is used to express both the spectra, their intersection gives the site-specific performance point of the building. However, site-specific demand spectrum obtained in Section 2.1 is for 5% viscous damping of the building. According to ATC 40 [19], effective damping (β_{eff}) of the building during earthquake excitation is combination of viscous damping that is inherent in the building (about 5%) and hysteretic damping (β_o) that is related to the area inside the hysteretic loops formed when the earthquake force is plotted against the structural displacement. In view of this, it is proposed to modify the demand spectrum obtained in Section 2.1 to account for the effective damping of the structure. Inelastic deformation undergone by the building, which is given by the distance between the yield point and the performance point, is a measure of effective damping of the structure. Eventually, this presents a nonlinear relation between effective damping and the demand spectrum. An iterative method (Fig. 2) consisting of sequence of simple calculations is suggested for solving the nonlinear relation. Demand spectrum has to be updated in each iterative cycle till convergence is achieved. Two procedures (P1 and P2) as suggested by ATC 40 [19] and FEMA 440 [4], respectively, are adopted in the proposed methodology to determine the hysteretic damping of the structure due to inelastic deformation. By applying one of the procedures, it is proposed to compute an updated value of hysteretic damping in each cycle which in turn can be used to evaluate effective damping of the building.

2.3.1. Procedure 1 (P1)

Capacity spectrum method of ATC 40 [19] assumes that the maximum displacement of a nonlinear SDOF system can be estimated from the maximum displacement of a linear elastic SDOF system which has an equivalent period and damping ratio. Hysteretic damping value (β_o) in percentage is obtained from the yield point and performance point ordinates in an iteration using Eq. (5) [19]

$$\beta_o = \frac{63.7(a_y d_{pi} - d_y a_{pi})}{a_{pi} d_{pi}} \tag{5}$$

where a_y=spectral acceleration at yield; d_y=spectral displacement at yield; a_{pi}=spectral acceleration at ith iteration; d_{pi}=spectral displacement at ith iteration.
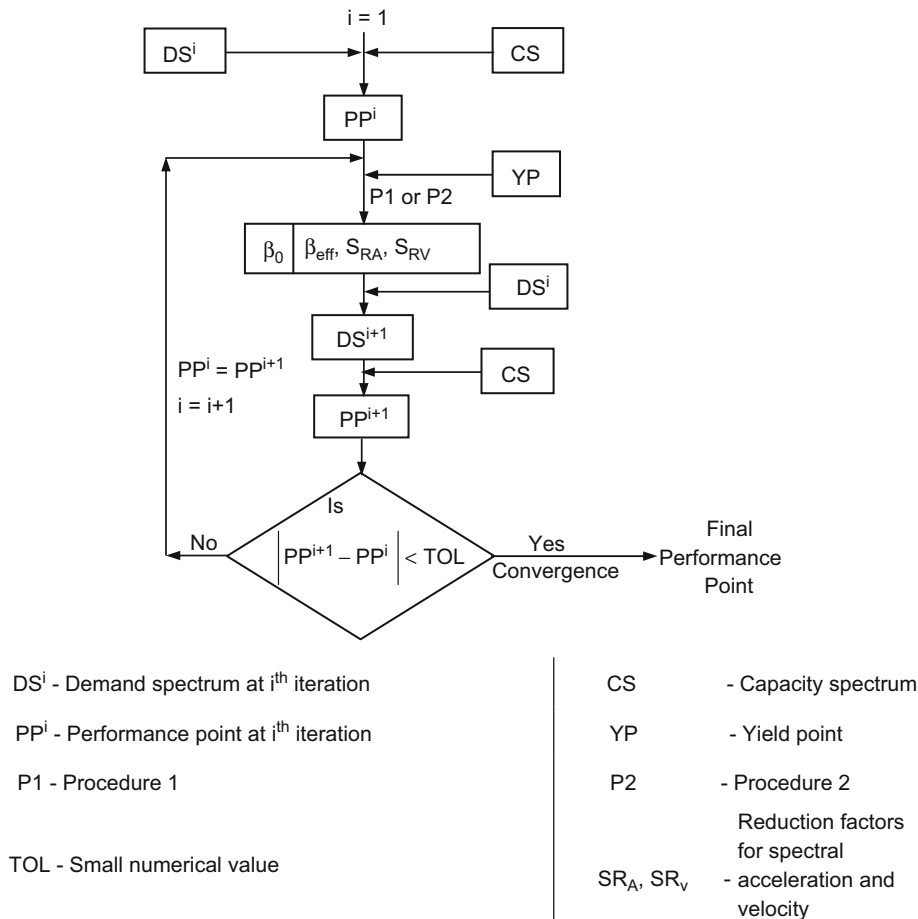
Fig. 2. Iterative procedure to find the performance point.

2.3.2. Procedure 2 (P2)

The equivalent period and equivalent damping can also be computed from the maximum displacement ductility ratio, μ [4,33]. Hysteretic damping (β_o) is calculated using the Eq. (6) and the performance point is calculated in several steps based on a bilinear model (Fig. 3).

$$\beta_o = 63.7 \left[\frac{(1-\alpha_i)(\mu_i-1)}{(\mu_i-\alpha_i\mu_i+\alpha_i\mu_i^2)} \right] \qquad (6)$$

where, $\mu_i=\delta_i/\delta_y$ is ductility at ith iteration; δ_y – displacement at yield; δ_i –displacement at ith iteration; $\alpha_i=k_i/k_y$ is post-elastic stiffness ratio at ith iteration; k_i – stiffness at ith iteration; k_y – elastic stiffness.

2.3.3. Modified effective damping (β_{eff})

To account for the structural behaviour of an existing reinforced concrete building, β_{eff} is proposed to be modified by using a damping factor κ (Eq. (7)) [19,4] which depends solely on the expected structural behaviour of the building. Guidelines to choose the numerical value of κ are available in Refs. [4,19].

$$\beta_{eff} = \kappa\beta_o + 5 \qquad (7)$$

2.3.4. Reduction of 5 per cent demand spectrum

Converged effective damping value is proposed to be used to estimate the spectral reduction factors, SR_A and SR_V, using the following relations [19,4],

$$SR_A = \frac{3.21-0.68\ln(\beta_{eff})}{2.12} \qquad (8)$$
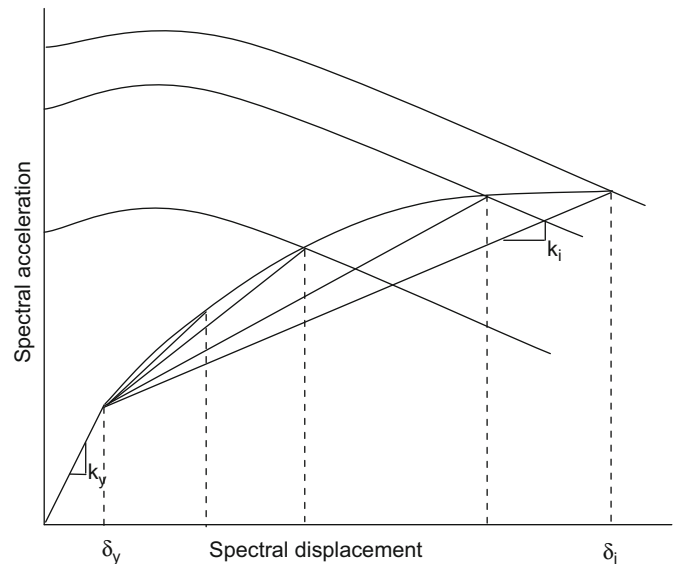
Fig. 3. Bi-linear modelling for damping calculation.

$$SR_V = \frac{2.31-0.41\ln(\beta_{eff})}{1.65} \qquad (9)$$

The computed factors are to be subjected to their minimum values as given by ATC 40 [19]. In each iterative cycle, the demand spectrum has to be successively scaled using the spectral reduction factor. For acceleration dominated region of DDDS,

the factor SR_A has to be used for scaling while the factor SR_V has to be used for scaling the velocity dominated region. Difficulty lies, however, due to the fact that DDDS does not have clearly identifiable regions that are controlled predominantly by acceleration or velocity unlike the design spectrum suggested by a code. It is, however, proposed that DDDS up to the natural period of the site can be considered as acceleration predominant region and the remaining can be considered as velocity predominant for the purpose of scaling the demand spectrum.

3. Demonstration of the methodology

In order to demonstrate the methodology, two buildings designated as B1 and B2 are chosen. Both the buildings are assumed to be located on different depths of soil strata at Delhi to calculate the performance points using the proposed methodology.
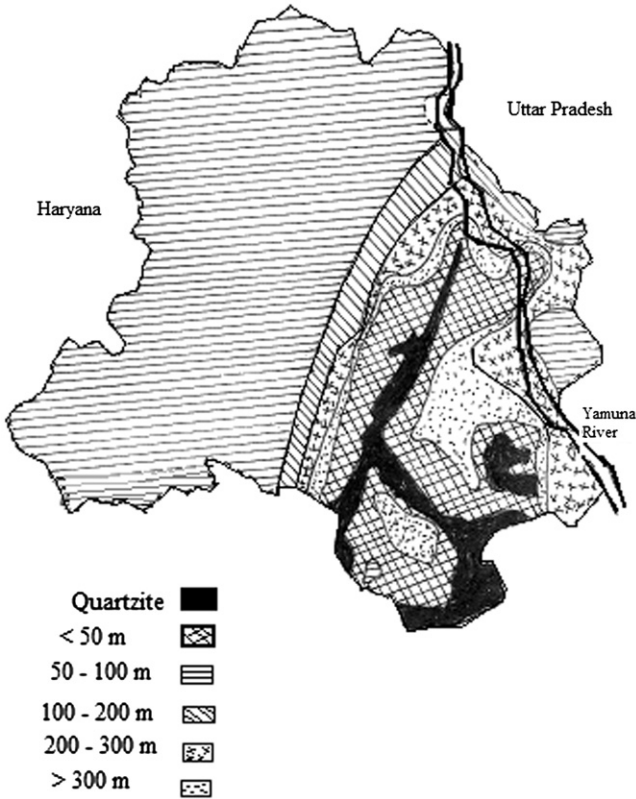
Fig. 4. Thickness of soil stratum above bedrock for Delhi region.

Table 2
Time periods of soil strata.

Sl. No.	Depth of soil stratum (m)	Time period (s)
1	10	0.19
2	20	0.34
3	30	0.47
4	50	0.67
5	75	0.9
6	100	1.2
7	150	1.6
8	200	2.0

3.1. Generation of demand curve

Generation of demand curve for site-specific earthquake is a major task towards applying the methodology. For this purpose, artificial ground motions are generated for Delhi region for a scenario earthquake of moment magnitude 8.5 originating from Central Seismic Gap (CSG) of Himalayan region. According to seismologists [26,34,35] the probability of occurrence of an earthquake of moment magnitude 8.5 in next 100 years at CSG is 0.59. Risk level corresponding to this is comparable with that of 50% exceedance in 100 years as specified in Indian seismic code 1893–2002 Part I [8]. No recorded ground motion with characteristics equivalent to the magnitude and distance considered for the scenario earthquake is available for Delhi. Hence, as described in an earlier section, finite source model proposed by Beresnev and Atkinson [23] has been used to generate artificial strong ground motion at reference site (Ridge observatory) for the scenario earthquake. For verification purpose, the generated ground motion is compared with that of Singh et al. [26] by the first author of this paper [36]. To account for the randomness in the simulation, 15 time history accelerations have been generated and used.

Next step is to propagate the earthquake generated for the reference site through different soil strata. Depth of soil stratum, shear wave velocity, modulus reduction curve and damping curve are the important properties that influence the modification of ground motion through soil layer. The thickness of alluvium above the bedrock at Delhi varies significantly and according to a report by Central Ground Water Board (CGWB) [37], variation is from less than 50 m to more than 300 m (Fig. 4). In the present study 8 representative soil strata defined by depths 10, 20, 30, 50, 75, 100, 150 and 200 m have been chosen. For shear wave
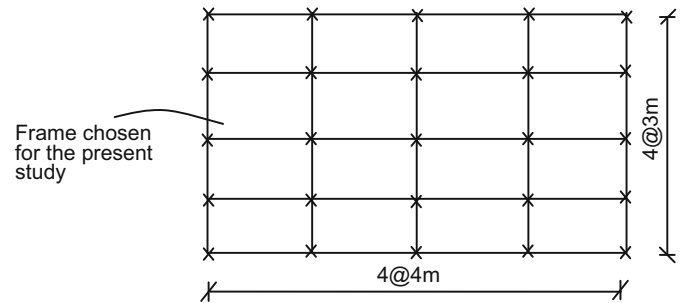
Fig. 5. Plan of the four storey building.
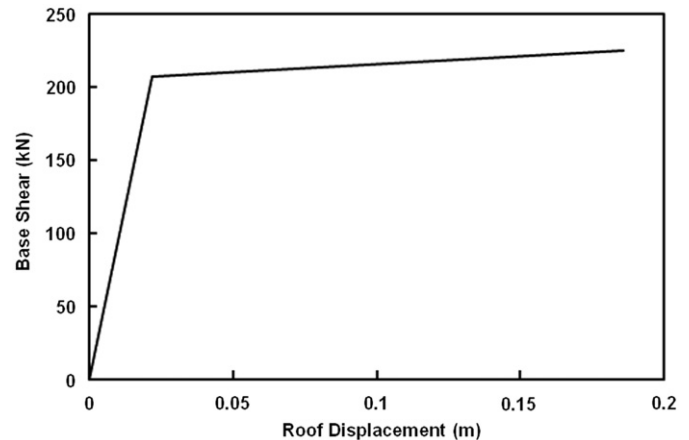
Fig. 6. Capacity curve of building B1.
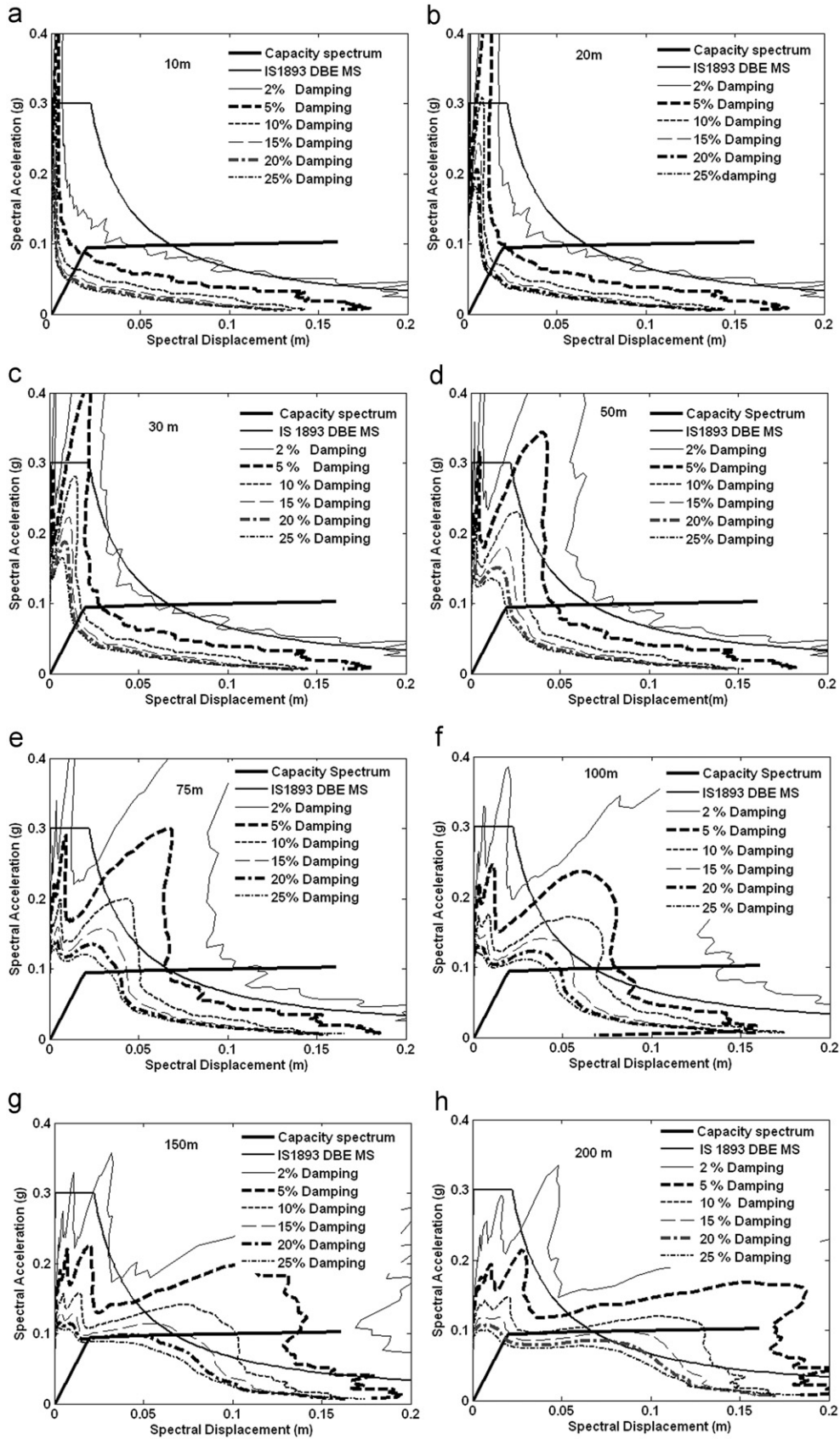
Fig. 7. Capacity and demand spectra for different damping ratios for B1.

velocity, regression relations (Eqs. (10)–(12)) have been suggested by Satyam [38] based on seismic refraction and Multi Array Surface Wave (MASW) tests. Delhi has been divided into three regions designated as M1, M2, M3.

$$V_s = 281 \ D_s^{0.08} \text{ for region M1} \tag{10}$$

$$V_s = 217 \ D_s^{0.13} \text{ for region M2} \tag{11}$$

$$V_s = 140 \ D_s^{0.24} \text{ for region M3} \tag{12}$$

where V_s = shear wave velocity in m/sec; D_s = depth of soil stratum in m;

The region M3 only has been considered for the present study. From the large number of borelog data available for Delhi region, it is observed that the Plasticity Index (PI) of soils at Delhi region varies from 0% to 15%. Modulus reduction curves and damping curves for Delhi soil corresponding to PI = 0% (Non plastic), PI = 15% (low plasticity) soil have been adopted from Vucetic and Dobry [39]. For rock, modulus reduction curves and damping curves have been chosen from Schnabel and Seed [40].

Ground motions are obtained at the top of representative soil sites by conducting equivalent linear one dimensional wave propagation analysis using the program SHAKE2000 [30]. The time periods of the 8 different soil stratum depths considered in the present study are given in Table 2. Using the surface ground motions, the average Depth Dependent Response Spectra (DDRS) of 15 random simulations of the ground motions at soil surface have been obtained corresponding to 2, 5, 10, 15, 20 and 25% damping.

3.2. Generation of capacity spectrum for B1

Initially nonlinear static analysis is carried out on building B1 and the capacity curves are generated using SAP2000 [32]. The building B1 is a four storey building with plan dimensions 16 m by 12 m as shown in Fig. 5. Beam and column dimensions and reinforcement details are adopted from Inel and Ozmen [41].

Considering the symmetry of the building and also neglecting torsion effects, 2-D model of an interior frame is chosen for the present study. The total height of the building is 11.2 m and typical floor-to-floor height is 2.8 m. The dead and participating live loads (30% of live load) on the frame are 197.6 and 36 tons, respectively.

The building is modelled with default PMM hinge properties for column and default M3 hinge properties for beam. The displacement control nonlinear static pushover analysis is carried out for the selected interior frame and the capacity curve of the building is obtained (Fig. 6). The capacity curve is transformed to capacity spectrum using Eqs. (3) and (4). The capacity spectrum is found to be nearly bilinear.

3.3. Generation of performance point for B1

The DDDS for eight different soil stratum depths and six different percentage damping values (2%, 5%, 10%, 15%, 20% and 25%), the demand curves as per 5% response spectra for medium soil design basis earthquake (DBE) of IS 1893–2002 [8] and the capacity spectrum are shown in Fig. 7 (a)–(h).

Though the DDDS has been generated for 6 different percentages of damping, the performance points are obtained corresponding to only 5% damping. However, spectral acceleration, S_a, spectral displacement, S_d, base shear V_b and top displacements Δ_{inel} at the intersection point of demand curve and capacity curve for different damping ratios are given in Tables 3 and 4. For the soil stratum depths 10 and 20 m, the demand curve corresponding to 5% damping intersects the capacity curve in elastic response region. For the other depths (30, 50, 75, 100 and 150 m), the intersection points lie in inelastic response region. For these depths the modified effective damping values and reduced demand spectra are obtained from 5% demand spectra using Procedure 1 (P1) and Procedure 2 (P2) described earlier (Eqs. (6)–(9)). The computed results are shown in Fig. 8 (a)–(j). Even though it is sufficient to use either procedure P1 or

Table 3
S_a, S_d, V_b and Δ_{inel} for 2%, 5% and 10% damping for B1.

Depth of soil stratum (m)	2%				5%				10%			
	S_a (g)	S_d (m)	V_b (kN)	Δ_{inel} (m)	S_a (g)	S_d (m)	V_b (kN)	Δ_{inel} (m)	S_a (g)	S_d (m)	V_b (kN)	Δ_{inel} (m)
10	0.098	0.051	214.678	0.056	0.086	0.018	188.244	0.020	0.063	0.014	136.656	0.016
20	0.098	0.055	212.931	0.060	0.099	0.022	216.539	0.024	0.071	0.016	155.114	0.018
30	0.100	0.060	218.609	0.065	0.096	0.029	208.782	0.031	0.086	0.020	187.087	0.021
50	0.096	0.077	209.841	0.085	0.098	0.048	213.434	0.052	0.097	0.032	211.359	0.035
75	0.100	0.105	218.810	0.114	0.101	0.065	221.261	0.070	0.098	0.051	213.608	0.056
100	0.102	0.140	223.038	0.153	0.099	0.080	216.276	0.087	0.096	0.069	210.573	0.076
150	–	–	–	–	0.104	0.137	227.886	0.150	0.098	0.102	213.761	0.112
200	–	–	–	–	–	–	–	–	0.097	0.032	212.058	0.035

Table 4
S_a, S_d, V_b and Δ_{inel} for 15%, 20% and 25% damping for B1.

Depth of soil stratum (m)	15%				20%				25%			
	S_a (g)	S_d (m)	V_b (kN)	Δ_{inel} (m)	S_a (g)	S_d (m)	V_b (kN)	Δ_{inel} (m)	S_a (g)	S_d (m)	V_b (kN)	Δ_{inel} (m)
10	0.063	0.014	136.669	0.016	0.094	0.049	204.768	0.054	0.094	0.043	205.219	0.047
20	0.062	0.015	134.900	0.016	0.060	0.012	130.292	0.013	0.055	0.013	120.530	0.014
30	0.076	0.017	166.108	0.018	0.068	0.016	149.506	0.017	0.067	0.015	145.361	0.016
50	0.093	0.026	203.762	0.028	0.091	0.023	198.041	0.025	0.091	0.020	199.703	0.022
75	0.096	0.043	209.437	0.047	0.098	0.038	214.089	0.042	0.091	0.025	199.701	0.028
100	0.094	0.056	206.052	0.062	0.094	0.049	204.768	0.054	0.094	0.043	205.219	0.047
150	0.100	0.072	218.107	0.078	0.094	0.023	205.191	0.026	0.089	0.019	194.743	0.021
200	0.092	0.022	200.068	0.024	0.087	0.019	189.286	0.021	0.081	0.018	177.523	0.019

P2, two sets of results were obtained by using both these procedures independently. Both the result sets are presented in Fig. 8 (a)–(j) to make a meaningful comparison among them. The trial performance points, led to the modification of effective damping (β_{eff}) and spectral reduction factors (SR_A and SR_v). Base shear and top displacement corresponding to the final performance point are given in Table 5. The Indian seismic code spectra intersect the capacity curve in the inelastic region. The modification has been carried out for effective damping as per procedures P1 and P2. The site-specific base shear and top

displacement (which includes the effects of soil amplification) corresponding to different depths of soil strata along with those due to DBE of IS 1893-2002 Part I [8] are given in Table 6. It may be noted that two sets of base shear and top displacement values have been calculated corresponding to procedures P1 and P2.

3.4. Generation of capacity spectrum for B2

Plan of building B2 is shown in Fig. 9. Overall length and width of the building are 11.4 and 10.9 m, respectively. Height of the
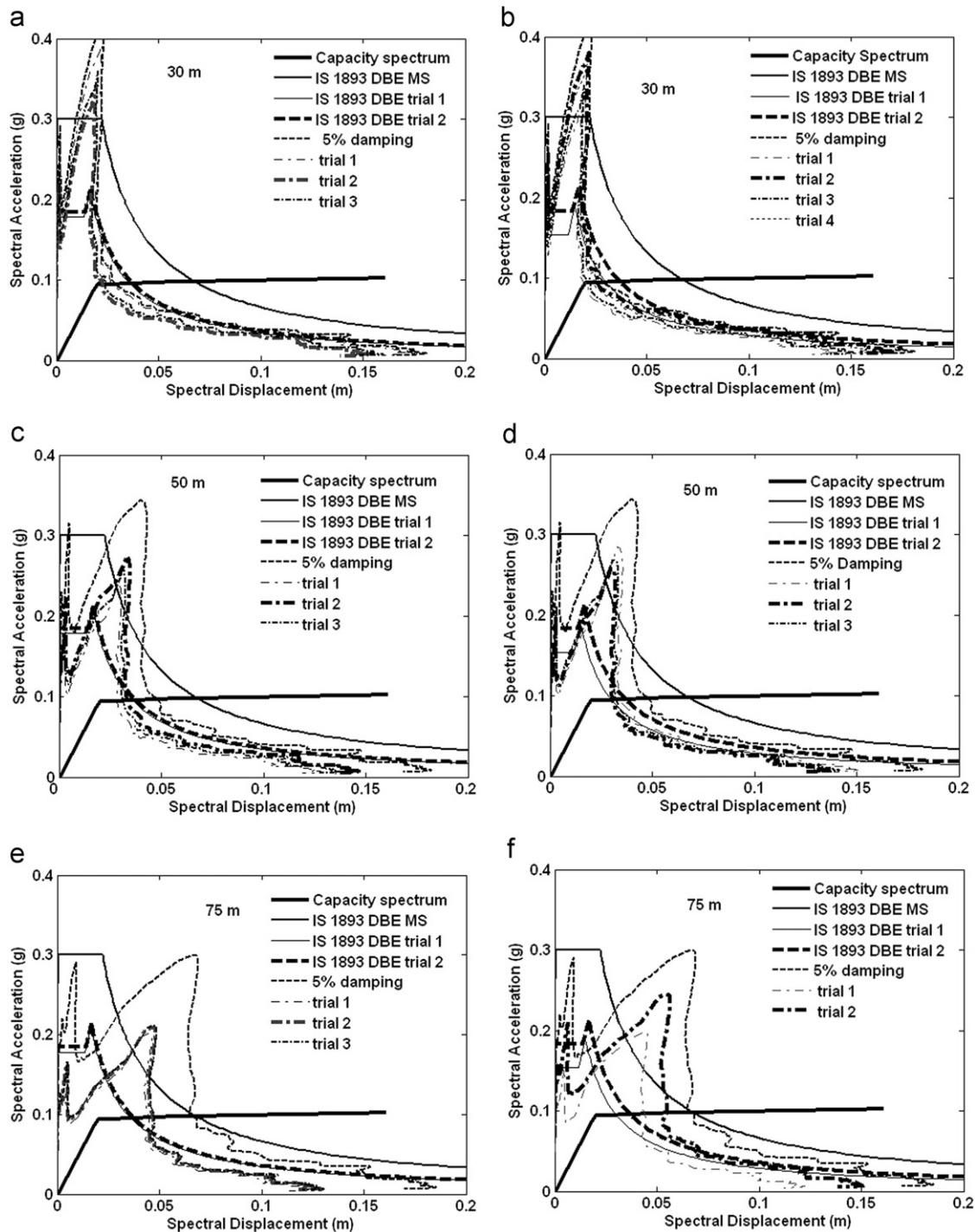
Fig. 8. Performance points using procedures P1 (a, c, e, g, i) and P2 (b, d, f, h, j) for different soil stratum depths, DDDS and IS 1893-2002 medium soil demand spectra for B1.
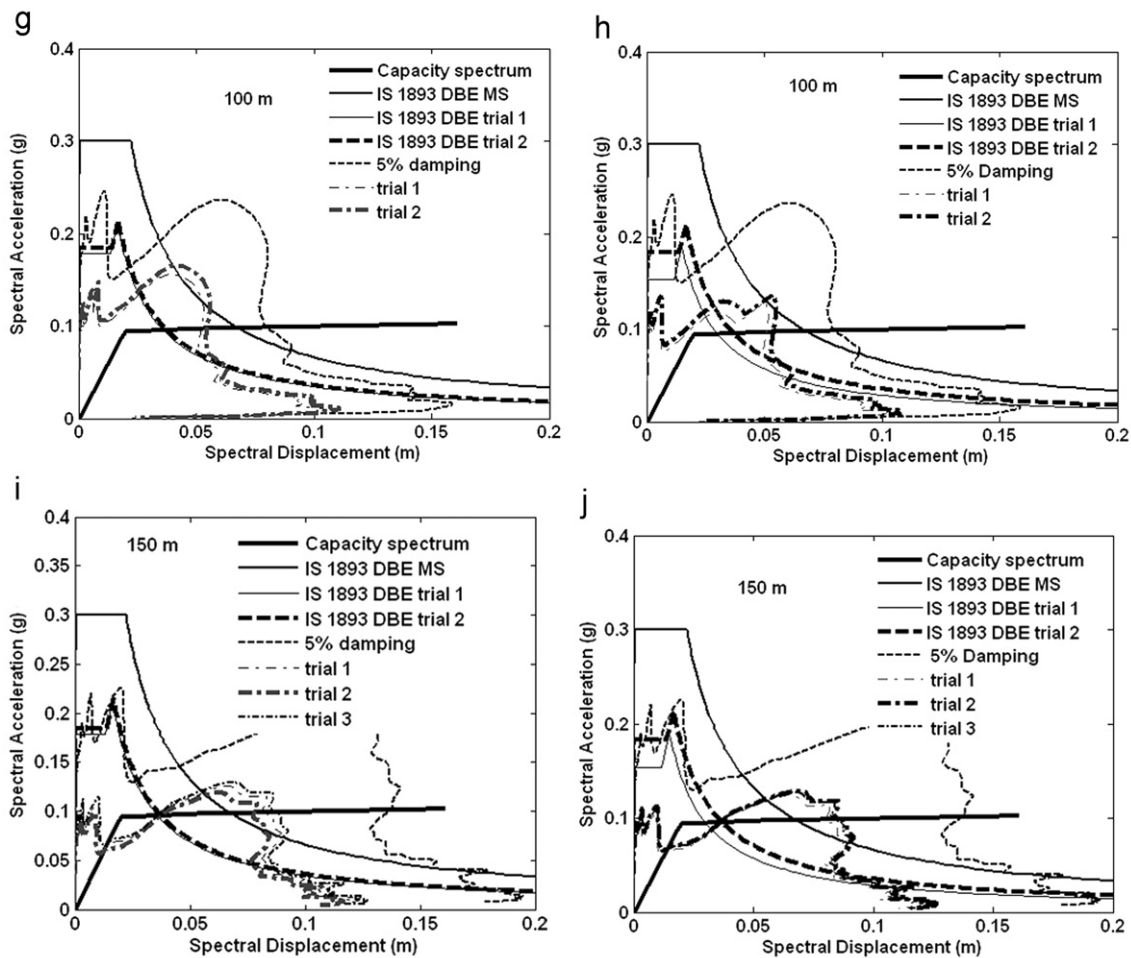
Fig. 8. (*Continued*)

Table 5
S_a, S_d, V_b and Δ_{inel} for reduced demand spectra for B1.

Depth of soil stratum (m)	P1				P2			
	S_a (g)	S_d (m)	V_b (kN)	Δ_{inel} (m)	S_a (g)	S_d (m)	V_b (kN)	Δ_{inel} (m)
30	0.0961	0.0238	209.96	0.0260	0.0232	0.0934	204.03	0.0254
50	0.0970	0.0319	211.91	0.0349	0.0312	0.0949	207.25	0.0341
75	0.0972	0.0474	212.32	0.0518	0.0546	0.0976	213.08	0.0596
100	0.0965	0.0540	210.68	0.0590	0.0533	0.0952	207.80	0.0581
150	0.0985	0.0885	215.07	0.0966	0.0839	0.0986	215.26	0.0916

Table 6
Comparison of V_b and Δ_{inel} for reduced spectra with DBE for B1.

Depth of soil stratum (m)	P1						P2					
	V_b (kN)			Δ_{inel} (m)			V_b (kN)			Δ_{inel} (m)		
	Site-specific	DBE	% difference*	Site-specific	DBE	% difference*	Site-specific	DBE	% difference*	Site-specific	DBE	% difference*
30	209.96	202.03	3.93	0.026	0.0425	−38.82	204.03	202.16	0.93	0.025	0.0529	−51.98
50	211.91	202.03	4.89	0.035	0.0425	−17.88	207.25	202.16	2.52	0.034	0.0529	−35.54
75	212.32	202.03	5.09	0.052	0.0425	21.88	213.08	202.16	5.40	0.060	0.0529	12.67
100	210.68	202.03	4.28	0.059	0.0425	38.82	207.8	202.16	2.79	0.058	0.0529	9.83
150	215.07	202.03	6.45	0.097	0.0425	127.29	215.26	202.16	6.48	0.092	0.0529	73.16

* Positive values indicate site-specific analysis results are higher
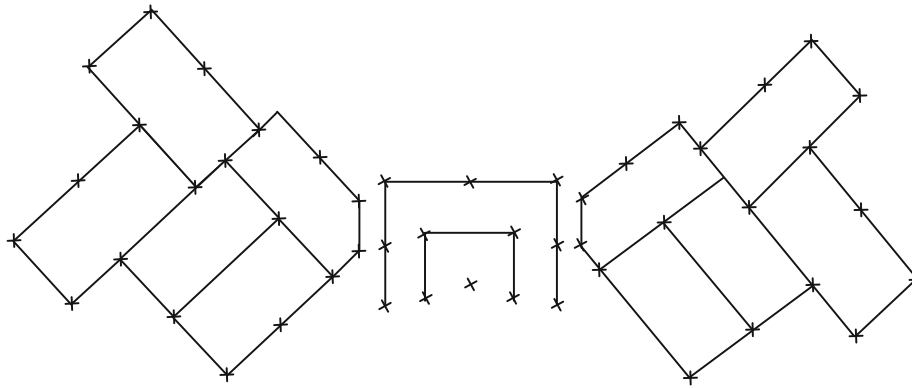
Fig. 9. Plan of building B2.
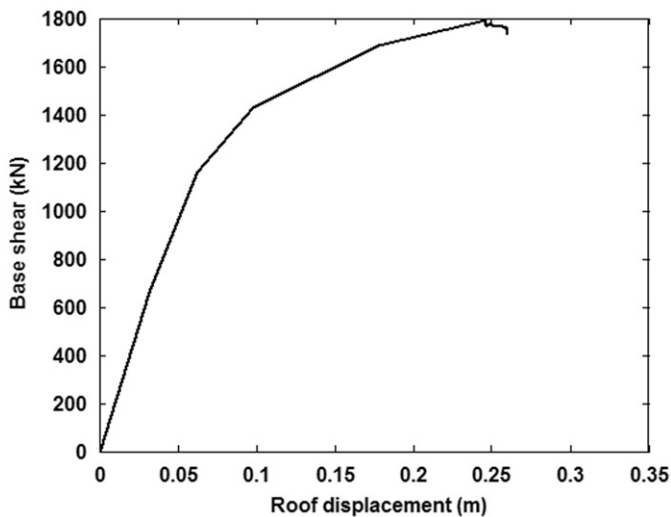
Fig. 10. Capacity curve of building B2.

building is 23.6 m. Cross section and reinforcement details of the beams and columns are modelled as given in the construction drawings of the building. The total lumped mass due to dead and participating live loads of the building for the bottom six stories is equal to 179.2 tons while the lumped mass for seventh and eighth stories is equal to 90.1 and 17.9 tons, respectively. This building has been modelled with 18 different sets of section properties. The details of the section properties are not included in the paper. The same can be obtained by contacting the authors.

Building B2 has been modelled using SAP2000 [32], with default PMM hinge properties for column and default M3 properties for beam. Displacement controlled nonlinear static pushover analysis has been carried out for the 3D building model and the capacity curve of the building (Fig. 10) is obtained. Further, the capacity curve is transformed to capacity spectrum using Eqs. (3) and (4).

Capacity and demand curves for the eight different depths of soil stratum are obtained for building B2 and shown in Fig. 11 (a)–(h). The intersection points of demand curve and capacity curve for different damping ratios, the base shear and top displacements for B2 are given in Tables 7 and 8. For the soil stratum depths of 10, 20, 30, 50 and 200 m, the 5% demand curve intersect the capacity curve in the elastic response region. For the other depths (75, 100 and 150 m), the intersection points are found to lie in inelastic response region. For these three depths, spectral

reduction factors are applied to 5% demand spectra and the performance points are obtained using procedures P1 and P2. This is carried out through number of trials as shown in Fig. 12 (a)–(f). The trial performance points are arrived at by using β_{eff}, SR_A and SR_v corresponding to soil stratum depths of 75, 100 and 150 m. The base shear and roof displacements corresponding to the final performance points of B2 for different depths of soil stratum are compared in Table 9. As like for building B1, the site-specific base shear and top displacement for different soil stratum depths are compared with corresponding values due to IS 1893–2002 DBE [8] in Table 10. Based on reasons explained already in the context of building B1, two sets of results are obtained by using both the procedures independently.

4. Discussions

Methodology proposed in this paper has clearly brought out the effect of local soil and depth of soil stratum on the seismic performance of building. For building B1, maximum percentage difference in base shear and top displacement is 6.45% and 127.3% as per P1 and 6.45% and 73.16% as per P2, respectively. It is apparent that for a nearly perfect elasto-plastic system as in the case of B1, the base shear demand remains constant in the inelastic region since S_a/g is a constant. However, the performance point is strongly dependent on time period, and ductility (or) estimate of equivalent damping due to inelastic deformations. The displacement demand is significantly different for M3 soil strata for depths in excess of 75 m. The variation of the percentage increase in displacement demand with depth of soil was nearly quadratic (proportional to square of soil depth) for the building B1. While the structure chosen is highly ductile with displacement ductility in the order of 7.0, majority of the structures built using normal detailing provisions may have displacement ductility ranging from 2.0 to 4.0. It is apparent that for depths in excess of 75 m, such structures are likely to fall short of inelastic displacement demand, even though code provisions may indicate the existence of a performance point.

The capacity curve for building B2 is typical of majority of framed structures with multiple reductions in stiffness levels in the post-yield scenario. This case more or less depicts the converse scenario of building B1. In this case, a number of buildings having different capacity curves may show a nearly constant spectral displacement, but may have a highly variable spectral acceleration demand. When compared to the spectra of IS 1893–2002 [8], maximum percentage difference in base shear and top displacement for 100 m depth is 48.8% and 89.8%, respectively, as per P1 and 52% and 94%, respectively, as per P2.

The ratio of percentage increase in spectral displacement to percentage increase in spectral acceleration or base shear demand was approximately 1.8 for the case of 100 m soil depth. The spectral displacement demand for depths in excess of 75 m varied in a narrow range of 0.071–0.095 m with a mean value of 0.083 m.

However, for systems with continuous variation in capacity spectrum, the depth of soil stratum has influence on the base shear demand as well as the inelastic displacement demand. For a given capacity curve the ratio of increase in displacement demand to increase in shear demand is likely to be a constant as the soil-amplification curves show vertical drop from a peak (S_a/g) value to a low (S_a/g) value at a constant S_d.

5. Summary and conclusions

A methodology is proposed for seismic performance evaluation of an existing building for site-specific earthquake and it is demonstrated for Delhi region. Artificial ground motions at rock outcrop are generated for a scenario earthquake of $M_w = 8.5$. The modified ground motions on top of different depths of representative soil stratum are evaluated. The DDDS for 5% damping ratio are obtained for eight different assumed depths of soil stratum above bedrock. The capacity curves of two buildings B1 and B2 are obtained. Subsequently, the modified effective damping values are evaluated using two procedures P1 and P2. The base shear and roof displacements of B1 and B2 for response spectra of site-specific scenario earthquake and spectra of the DBE of Indian seismic code are compared.

For building B1 which has nearly elasto-plastic behaviour, with soil stratum depths of 30, 50, 75, 100 and 150 m, the 5% demand curve intersect the capacity curve in the inelastic region. For 200 m depth 5% demand curve does not intersect the capacity curve. For soil stratum depths above 75 m, the inelastic displacements are more than that of the DBE of IS 1893–2002 [8] DBE. The results indicate that the depth of soil stratum has significant influence on displacement demand compared to base shear demand in buildings which can be idealized as elasto-plastic. For building B2 which has continuously varying inelastic behaviour, with soil stratum depths of 75, 100 and 150 m, the 5% demand curve intersect the capacity curve in the inelastic region. For remaining depths studied, demand curve intersect the capacity curve within the elastic region. Indian seismic code spectra intersect the capacity curve in the elastic region and hence damping modification has not been applied to code spectra for B2. The results indicate that for buildings with continuous variation in capacity spectrum, the depth of soil stratum has influence on the base shear demand as well as on the inelastic displacement demand.

From the studies made, it is clear that considering the design spectra suggested by seismic codes and only the top 30 m soil stratum to include the effects of soil amplification may not ensure safe seismic performance of a building. It is further seen that the site-specific earthquake and the depth of soil stratum have significant influence on the performance of the building both in terms of inelastic displacement as well as inelastic base shear.
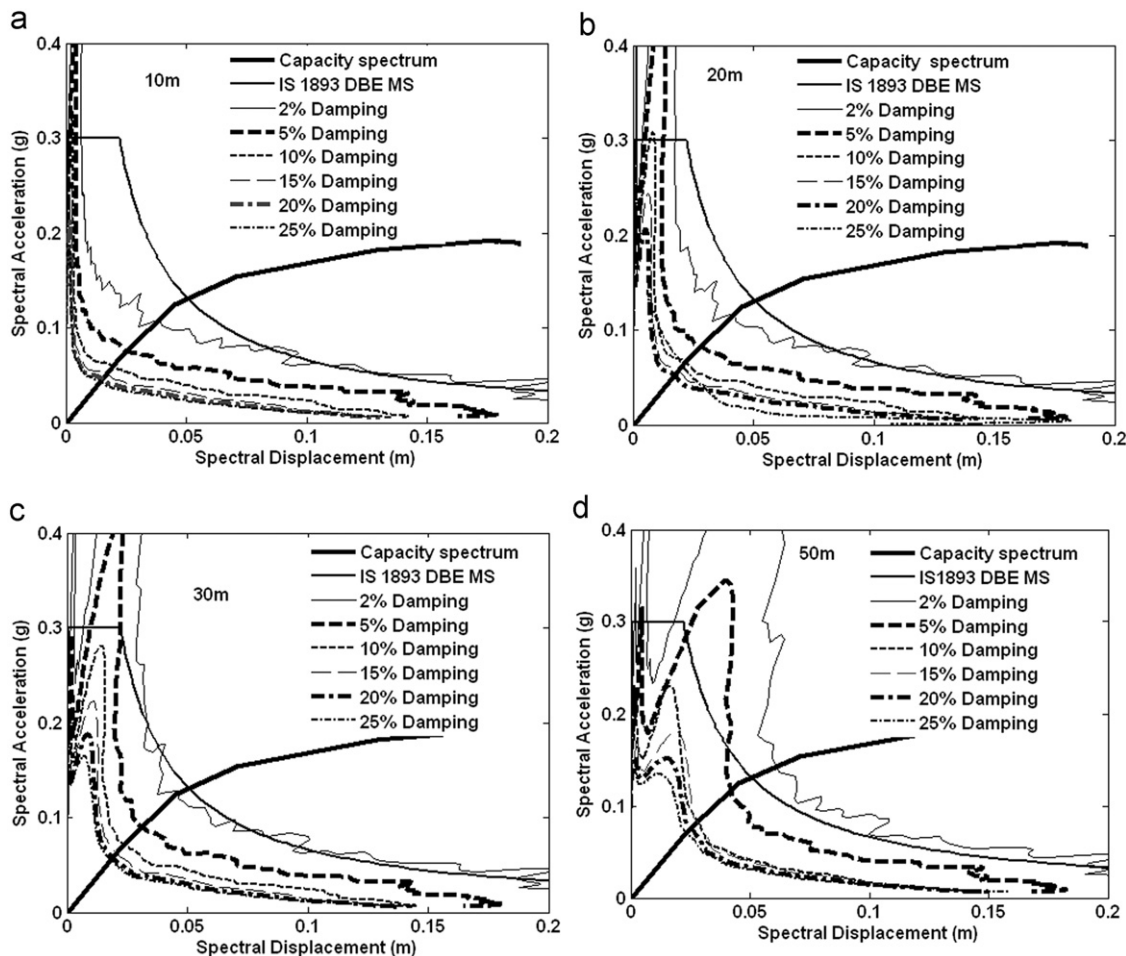
Fig. 11. Capacity and demand spectra for different damping ratios for B2.
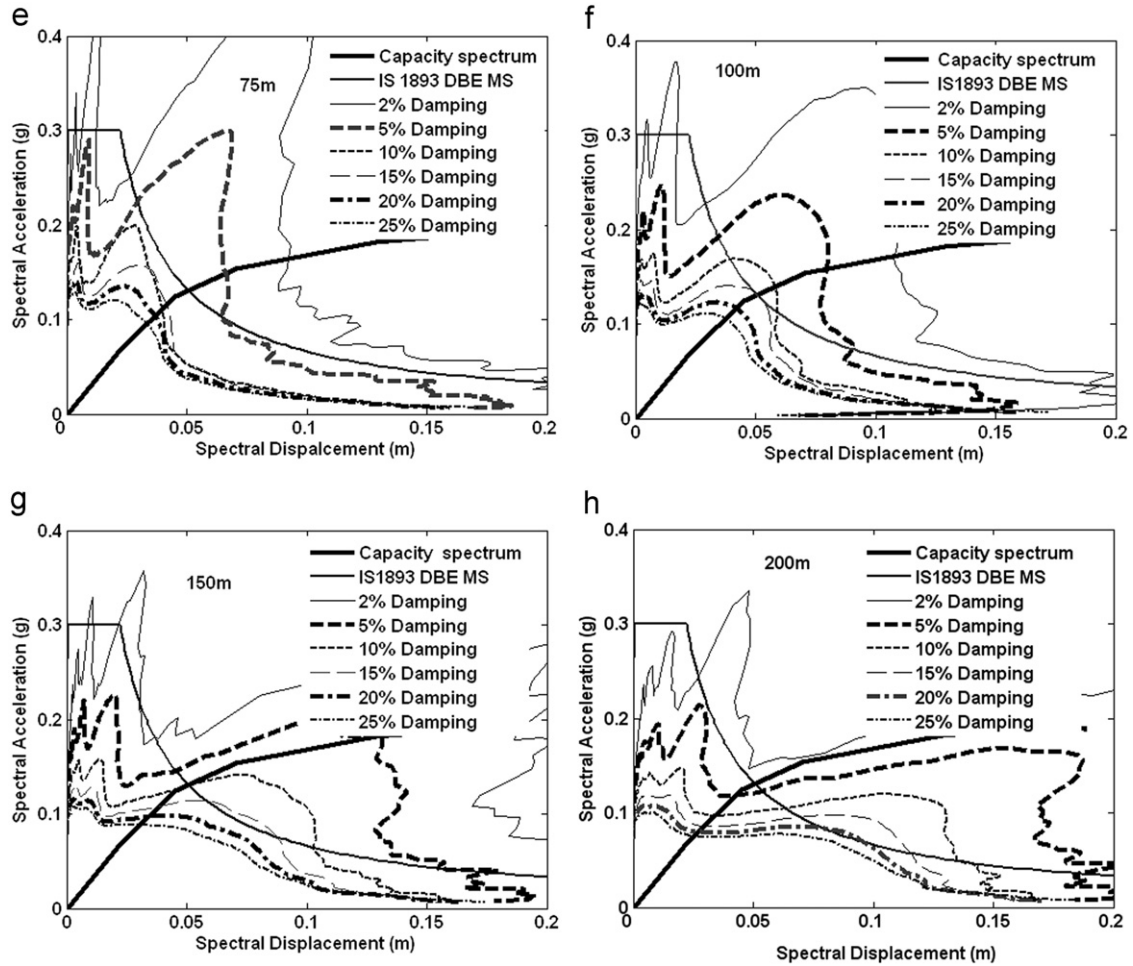
Fig. 11. (Continued)

Table 7
S_a, S_d, V_b and Δ_{inel} for 2%, 5% and 10% damping for B2.

Depth of soil stratum (m)	2%				5%				10%			
	S_a (g)	S_d (m)	V_b (kN)	Δ_{inel} (m)	S_a (g)	S_d (m)	V_b (kN)	Δ_{inel} (m)	S_a (g)	S_d (m)	V_b (kN)	Δ_{inel} (m)
10	0.1087	0.0390	1009.3447	0.0538	0.0759	0.0250	704.7678	0.0345	0.0595	0.0196	552.8767	0.0270
20	0.1172	0.0420	1087.9938	0.0579	0.0834	0.0274	774.5026	0.0379	0.0658	0.0216	611.0481	0.0299
30	0.1283	0.0460	1191.4415	0.0634	0.0921	0.0303	855.5752	0.0418	0.0722	0.0238	670.7546	0.0328
50	0.1447	0.0608	1344.0409	0.0840	0.0977	0.0476	213.4335	0.0520	0.0968	0.0318	211.3588	0.0348
75	0.1654	0.0926	1536.1902	0.1278	0.1954	0.0653	1814.2939	0.0901	0.1370	0.0491	1272.033	0.0677
100	0.1632	0.1078	1515.7813	0.1488	0.1636	0.0798	1519.5411	0.1101	0.1464	0.0569	1359.411	0.0785
150	–	–	–	–	0.1813	0.1228	1683.9055	0.1695	0.1256	0.0450	1166.376	0.0621
200	–	–	–	–	0.1192	0.0427	1106.3792	0.0589	0.0968	0.0347	898.8368	0.0478

Table 8
S_a, S_d, V_b and Δ_{inel} for 15%, 20% and 25% damping for B2.

Depth of soil stratum (m)	15%				20%				25%			
	S_a (g)	S_d (m)	V_b (kN)	Δ_{inel} (m)	S_a (g)	S_d (m)	V_b (kN)	Δ_{inel} (m)	S_a (g)	S_d (m)	V_b (kN)	Δ_{nel} (m)
10	0.0595	0.0196	552.8646	0.0270	0.0533	0.0184	494.8853	0.0254	0.0422	0.0151	391.8152	0.0209
20	0.0526	0.0198	487.9583	0.0273	0.0526	0.0173	487.9583	0.0239	0.0526	0.0173	487.9583	0.0239
30	0.0582	0.0192	540.6689	0.0264	0.0557	0.0183	516.9479	0.0253	0.0557	0.0183	516.9479	0.0253
50	0.0933	0.0256	203.7616	0.0279	0.0907	0.0226	198.0413	0.0246	0.0914	0.0201	199.7025	0.0219
75	0.1161	0.0416	1078.1818	0.0574	0.1032	0.0370	958.4223	0.0510	0.0834	0.0271	774.1126	0.0374
100	0.1313	0.0510	1218.8557	0.0704	0.1172	0.0420	1088.1795	0.0579	0.1054	0.0378	978.6837	0.0521
150	0.1087	0.3842	1008.9733	0.5302	0.0961	0.0356	892.3462	0.0491	0.0757	0.0289	702.8271	0.0399
200	0.0862	0.0284	800.6601	0.0391	0.0799	0.0263	741.4923	0.0363	0.0757	0.0249	702.8271	0.0344
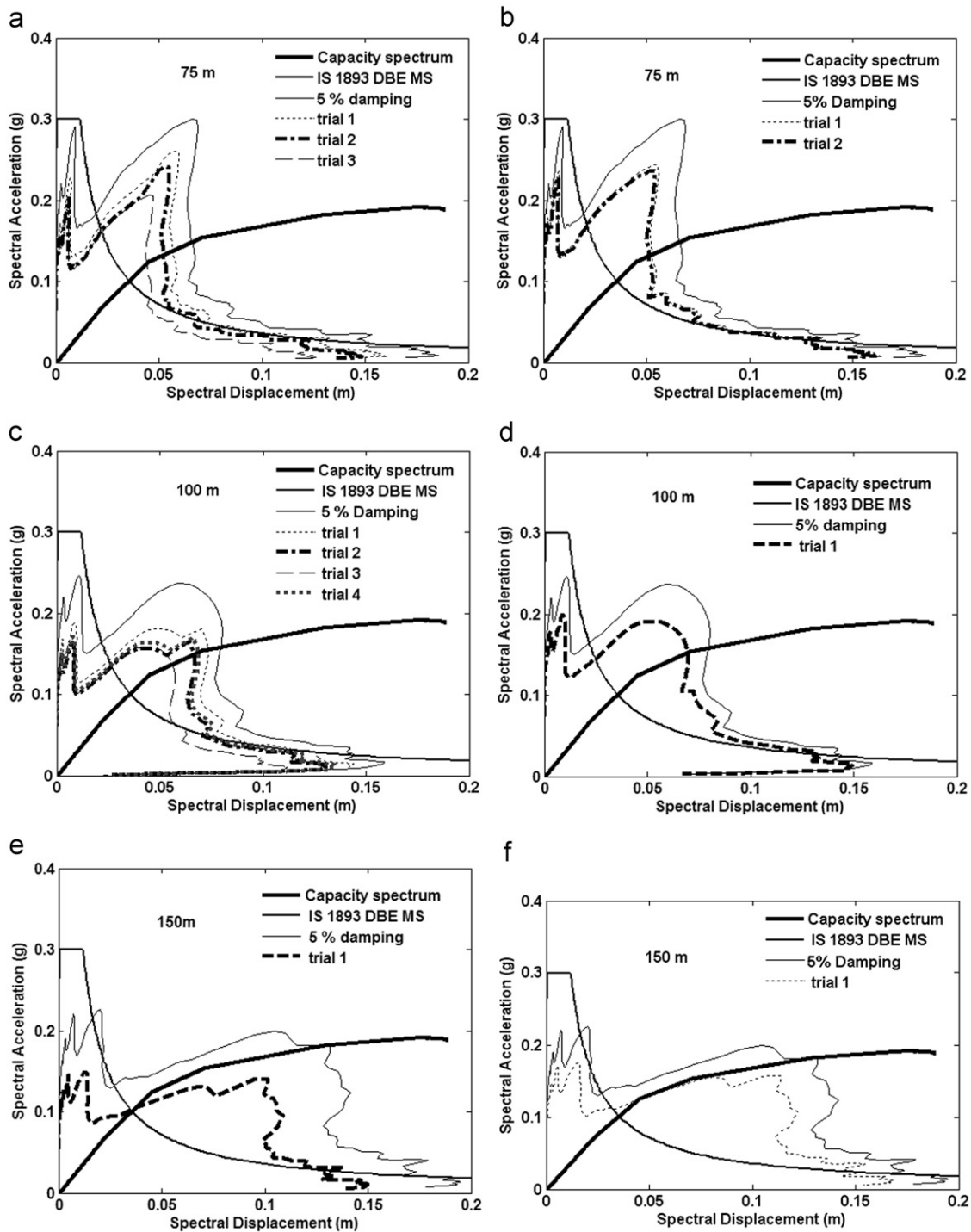
Fig. 12. Performance points using procedures P1 (a, c, e) and P2 (b, d, f) for different soil stratum depths, DDDS and IS 1893–2002 medium soil demand spectra for B2.

Table 9
S_a, S_d, V_b and Δ_{inel} for reduced demand spectra for B2.

Depth of soil stratum (m)	P1				P2			
	S_a (g)	S_d (m)	V_b (kN)	Δ_{inel} (m)	S_a (g)	S_d (m)	V_b (kN)	Δ_{inel} (m)
75	0.133	0.052	1235.91	0.071	0.129	0.050	1196.91	0.069
100	0.149	0.068	1381.70	0.093	0.152	0.069	1411.78	0.095
150	0.106	0.038	982.79	0.052	0.128	0.046	1186.38	0.063

Table 10
Comparison of V_b and $\varDelta_{inel}$ for reduced spectra with DBE for B2.

Depth of soil stratum (m)	P1						P2					
	V_b (kN)			$\varDelta_{inel}$ (m)			V_b (kN)			$\varDelta_{inel}$ (m)		
	Site-specific	DBE	% difference[a]	Site-specific	DBE	% difference[a]	Site-specific	DBE	% difference[a]	Site-specific	DBE	% difference[a]
75	1235.91	928.6	33.10	0.071	0.049	44.90	1196.91	928.6	28.89	0.0692	0.049	41.22
100	1381.7	928.6	48.79	0.093	0.049	89.80	1411.78	928.6	52.03	0.0951	0.049	94.08
150	982.79	928.6	5.84	0.052	0.049	6.12	1186.38	928.6	27.76	0.063	0.049	28.57

[a] Positive values indicate results of site-specific analysis are higher

References

[1] Fajfar P, Krawinkler H. Seismic design methodologies for the next generation of codes. Proceedings of the International Workshop on seismic design methodologies for the next generation of codes. Slovenia 1997.
[2] Midorikawa M, Okawa I, Iiba M, Teshigawara M. Performance-based seismic design code for buildings in Japan. Earth Eng Eng Seismology 2003;4(1): 15–25.
[3] Xue Q, Wu C-W, Chen C-C, Chen K-C. The draft code for performance based seismic design of buildings in Taiwan. Eng Struct 2008;30:1535–47.
[4] FEMA 440. Improvement of nonlinear static seismic analysis procedures. Appl Technol Counc (ATC 55 Project) Washington D.C. 2005.
[5] Stewart JP, Chiou S-J, Bray JD, Graves RW, Somerville PG, Abrahamson NA. Ground motion evaluation procedure for performance based design, PEER Report 2001/09, California, 2001.
[6] Stewart JP, Liu AH, Choi Y, Baturay MB. Amplification factors for spectral acceleration in active regions, PEER 2001/10, California, 2001.
[7] Ruiz-Garcia J, Miranda E. Inelastic displacement ratios for evaluation of existing structures. Earth Eng St Dyn 2003;32:1237–58.
[8] IS 1893-2002 (Part 1). Indian standard criteria for earthquake resistant design of structures. Part 1 – General Provisions and buildings, Bureau of Indian Standards, New Delhi.
[9] Borcherdt RD. Estimates of site-dependent response spectra for design methodology and justification. Earth Spect 1994;10(4):617–53.
[10] IBC. International Building Code. Washington D.C.: International Code Council; 2000.
[11] Elghazouli AY. Seismic design of buildings to Eurocode 8. Spon Press; 2009.
[12] Sun CG, Kim DS, Chung CK. Geologic site conditions and site coefficients for estimating earthquake ground motions in the inland areas of Korea. Eng Geol 2005;81(4):446–69.
[13] Heuze F, Archuleta R, Bonilla F, Day S, Doroudian M, Elgamal A, Gonzales S, Hoehler M, Lai T, Lavallee D, Lawrence B, Liu PC, Martin A, Matesic L, Minster B, Mellors R, Oglesby D, Park S, Riemer M, Steidl J, Vernon F, Vucetic M, Wagoner J, Yang Z. Estimating site-specific strong earthquake motions. Soil Dy Earth Eng 2004;24(3):199–223.
[14] Balendra T, Lam NTK, Wilson JL, Kong KH. Analysis of long-distance earthquake tremors and base shear demand for buildings in Singapore. Eng Struct 2002;24(1):99–108.
[15] Mammo T. Site-specific ground motion simulation and seismic response analysis at the proposed bridge sites within the city of Addis Ababa, Ethiopia. Eng Geol 2005;79(3-4):127–50.
[16] FEMA 273. NEHRP guidelines for the seismic rehabilitation of buildings. Washington D.C, 1997.
[17] FEMA 274. Commentary, Federal Emergency Management Agency, Washington D.C, 1996.

[18] FEMA 302. NEHRP recommended provisions for seismic regulations for new buildings and other structures, Part 1: Provisions, Federal Emergency Management Agency, Washington D.C, 1997.
[19] ATC 40. Applied Technology Council, Seismic evaluation and retrofit of concrete buildings, 1-2, California, 1996.
[20] Freeman SA. Review of the development of the capacity spectrum method. ISET Jl Earth Tech 2004;41(1):1–13.
[21] Boore DM. Stochastic simulation of high frequency ground motions based on seismological models of the radiated spectra Bull. Seism Soc Am 1983;73(6):1865–94.
[22] Boore DM. Simulation of ground motion using the stochastic method. Pure Appl Geophys 2003;160(3-4):635–76.
[23] Beresnev IA, Atkinson GM. Modeling finite – fault radiation from the ω^n spectrum. Bull Seism Soc Am 1997;87(1):67–84.
[24] Beresnev IA, Atkinson GM. FINSIM – a FORTRAN program for simulating stochastic acceleration time histories from finite faults. Seism Res Lr 1998;69(1):27–32.
[25] Atkinson GM, Beresnev IA. Ground motions at Memphis and St. Louis from M7.5-8.0 earthquakes in the New Madrid seismic zone. Bull Seism Soc Am 2002;92(3):1015–24.
[26] Singh SK, Mohanty WK, Bansal BK, Roonwal GS. Ground motion in Delhi from future large/great earthquakes in the central seismic gap of the Himalayan arc. Bull Seism Soc Am 2002;92(2):555–69.
[27] Pergalani F, Franco de, Compagnoni M, Caielli G. Evaluation of site effects using numerical and experimental analyses in Citta di Castello (Italy). Soil Dy Earth Eng 2006;26(10):941–51.
[28] Idriss IM. Response of soft soil sites during earthquakes. Proc. Symp. to Honor Prof. Seed H. B. Berkeley, California, 1990; 273–289.
[29] Schneider JF, Silva WJ, Stark C. Ground motion model for the 1989 M 6.9 Loma Prieta earthquake including effects of source, path, and site. Earth Spect 1993;9(2):251–87.
[30] SHAKE 2000. A computer program for the 1-d analysis of geotechnical earthquake engineering problems, user's manual. USA: University of California; 2006.
[31] Chopra AK, Goel RK. A modal pushover analysis procedure for estimating seismic demands for buildings. Earth Eng Struct Dy 2002;31:561–82.
[32] SAP2000. Linear and Nonlinear Static and Dynamic Analysis and Design of Three-dimensional Structures, Version 9.0. California, USA: Computers and Structures Inc.; 2004.
[33] Lakshmanan N. Seismic evaluation and retrofitting of buildings and structures Jl. of Indian Society for Earth. Tech 2006;43(1-2):31–48.
[34] Bilham R, Blume F, Bendick R, Gaur VK. The geodetic constrains on the translation and deformation of India: implication for future great Himalayan earthquakes. Curr Sci 1998;74(3):213–29.
[35] Khattri KN. An evaluation of earthquakes hazard and risk in northern India. Him Geol 1999;20:1–46.
[36] Kamatchi P. Neural network models for site-specific seismic analysis of buildings. Ph. D. Thesis, Department of Civil Engineering, Indian Institute of Technology Delhi; 2008.
[37] CGWB. Delhi environmental status report, Pollution Monitoring and Tech. Corp. Div., Central Ground Water Board, New Delhi 2002; 1.
[38] Satyam ND. Seismic microzonation studies for Delhi region, Ph. D. Thesis, Department of Civil Engineering, Indian Institute of Technology Delhi. 2006.
[39] Vucetic M, Dobry R. Effect of soil plasticity on cyclic response. J Geotech Eng ASCE 1991;117(1):89–107.
[40] Schnabel PB, Seed HB. Accelerations in rock for earthquakes in the Western United States. Report no. EERC 72-2, University of California, Berkeley, 1972.
[41] Inel M, Ozmen HB. Effects of plastic hinge properties in nonlinear analysis of reinforced concrete buildings. Eng Struct 2006;28:1494–502.